

See discussions, stats, and author profiles for this publication at: <https://www.researchgate.net/publication/231695739>

# In Vitro Monitoring of Poly(ortho ester) Degradation by Electron Paramagnetic Resonance Imaging

ARTICLE *in* MACROMOLECULES · JULY 2003

Impact Factor: 5.8 · DOI: 10.1021/ma034365q

---

CITATIONS

15

---

READS

30

8 AUTHORS, INCLUDING:



[Werner Herrmann](#)

Freie Universität Berlin

26 PUBLICATIONS 370 CITATIONS

SEE PROFILE



[Robert Gurny](#)

University of Geneva

366 PUBLICATIONS 14,610 CITATIONS

SEE PROFILE

## In Vitro Monitoring of Poly(ortho ester) Degradation by Electron Paramagnetic Resonance Imaging

Sergio Capancioni,<sup>†</sup> Khadija Schwach-Abdellaoui,<sup>†</sup> Werner Kloeti,<sup>‡</sup> Werner Herrmann,<sup>§</sup> Holger Brosig,<sup>§</sup> Hans-Hubert Borchert,<sup>§</sup> Jorge Heller,<sup>⊥</sup> and Robert Gurny<sup>\*,†</sup>

*School of Pharmacy, University of Geneva, Quai Ernest-Ansermet 30, 1211 Geneva 4, Switzerland;*

*Department of Mass Spectrometry, University of Geneva, 1211 Geneva 4, Switzerland;*

*Department of Pharmacy, Humboldt University of Berlin, 13086 Berlin, Germany; and*

*A.P. Pharma, Redwood City, California 94063*

*Received March 24, 2003; Revised Manuscript Received June 12, 2003*

**ABSTRACT:** Electron paramagnetic resonance (EPR) imaging was applied to investigate further the in vitro degradation process of poly(ortho esters) containing 30 mol % lactic acid units in the polymer backbone (POE<sub>70</sub>LA<sub>30</sub>) and developed for controlled drug delivery. The objective of this study was the direct and continuous determination of pH values inside the degrading POE<sub>70</sub>LA<sub>30</sub>. pH-sensitive nitroxide spin probes 4-amino-2,2,5,5-tetramethyl-3-imidazoline-1-yloxy, 2,2,3,4,5,5-hexamethylimidazolidine-1-yloxy, and 2,2,4,5,5-pentamethyl-3-imidazoline-1-yloxy were calibrated in buffer solutions in order to cover a pH range between 1.0 and 8.0. Nitroxide spin probes were incorporated in POE<sub>70</sub>LA<sub>30</sub>, and polymer samples were incubated in 0.1 M phosphate buffer (pH 7.4) at 37 °C. At selected times, polymer samples were removed for the determination of pH values inside the eroding POE<sub>70</sub>LA<sub>30</sub> by EPR at a frequency of 9.4 GHz. EPR imaging showed that the in vitro degradation of POE<sub>70</sub>LA<sub>30</sub> followed a two-phase process: in the first week of incubation, diffusion of water, and in consequence polymer degradation, were limited to the surface of the hydrophobic POE<sub>70</sub>LA<sub>30</sub> where pH values between 6.0 and 7.4 were measured. After 1 week of incubation, water diffused into the core of the sample, allowing the determination of pH values inside the eroding POE<sub>70</sub>LA<sub>30</sub> until complete erosion. Results indicated the formation of a pH gradient, with the most acidic environment inside the eroding sample where the lowest pH value of 3.8 was measured and higher pH at the surface. It was also possible to observe a polymer erosion front moving down within the polymer matrix in the course of time. The pH value of 3.8 measured inside the degrading POE<sub>70</sub>LA<sub>30</sub> remained constant until polymer samples disintegrated at day 23, where no EPR signal was detectable. In conclusion, EPR imaging allows the noninvasive spatially resolved observation of pH changes within POE<sub>70</sub>LA<sub>30</sub>, and results confirmed that the in vitro erosion mechanism of POE<sub>70</sub>LA<sub>30</sub> was neither bulk erosion nor pure surface erosion.

### Introduction

Bioerodible polymeric biomaterials made up of acidic monomers, such as poly( $\alpha$ -hydroxy esters), polyanhydrides, and poly(ortho esters), have become biomaterials of choice for the controlled release of active compounds. However, an acidic microenvironment can develop with time due to the accumulation of acidic byproducts inside the eroding polymer matrix. Therefore, quantifying the pH environment inside eroding polymeric drug delivery systems (DDS) is critical for furthering the understanding of polymer degradation and release kinetics and for optimizing the stability of the incorporated active compounds. Indeed, low pH values are known to be deleterious to active compounds such as proteins and nucleic acids and can trigger inflammatory reactions.<sup>1–6</sup> However, prediction of the pH inside DDS is difficult because factors such as polymer degradation and diffusion kinetics of the monomers into the release medium are known to be pH dependent. The analytical methods most frequently used for the characterization of biodegradable DDS include size exclusion chromatography, scanning electron microscopy, differential scanning cal-

orimetry, infrared spectroscopy, and the direct assessment of pH by glass electrodes.<sup>7,8</sup> All these methods require the destruction of the sample which increases the number of samples required and may lead to artifacts. Furthermore, they do not provide any spatial information concerning the degradation process. Although the importance of pH for polymer degradation and drug release kinetics is well documented, only certain techniques allow visualization of the spatial and temporal distribution of pH within eroding DDS. Confocal fluorescence microscopy was utilized by Shenderova et al. to show the existence of an acidic microenvironment within eroding poly(lactide-co-glycolide) microspheres.<sup>9</sup> In another study, Fu et al. entrapped pH-sensitive fluorescent dyes within PLGA microspheres, and results confirmed the formation of an acidic environment within the particles with pH values as low as 1.5.<sup>10</sup> The formation of acidic microenvironments is not surprising if we consider the bulk erosion process of poly( $\alpha$ -hydroxy esters). Nuclear magnetic resonance (NMR), a noninvasive technique widely used clinically as a diagnostic tool, can be used to characterize water penetration into DDS in vitro and in vivo. It was successfully applied by Mäder et al. for real-time measurements of water penetration into polyanhydride implants,<sup>11</sup> by Burke et al. to examine PLGA microspheres incubated in sheep serum,<sup>12</sup> and by Deutsch et al. for the measurement of intracellular pH.<sup>13</sup> Electron paramagnetic resonance spectroscopy

<sup>†</sup> School of Pharmacy, University of Geneva.

<sup>‡</sup> Department of Mass Spectrometry, University of Geneva.

<sup>§</sup> Humboldt University of Berlin.

<sup>⊥</sup> A.P. Pharma.

\* To whom correspondence should be addressed: phone +41.22.379.61.46; Fax +41.22.379.65.67; e-mail Robert.Gurny@pharm.unige.ch.

(EPR, or equivalent electron spin resonance, ESR) shows great potential in the pharmaceutical sciences for the characterization of systems containing endogenous paramagnetic species.<sup>14,15</sup> The characterization of systems that are made up of only diamagnetic species is only possible after the introduction of exogenous paramagnetic compounds, i.e., spin probes, acting as molecular probes. As an example, spin probes have been used successfully to monitor water penetration into biodegradable polymers.<sup>16,17</sup> A novel application was made possible by the synthesis of pH-sensitive nitroxide spin probes.<sup>18</sup> The protonation of groups localized near the nitroxyl moiety induces changes of the spin density on the nitrogen atom of the radical nitroxyl group, leading to changes in spectroscopic parameters such as the hyperfine splitting ( $a_N$ ) and  $g$ -factor. This noninvasive technique has been used to study proton transport across phospholipid membranes<sup>19,20</sup> and diffusion of acid molecules in viscous glycerol/water mixtures<sup>21</sup> and for the direct and continuous measurement of pH values inside DDS.<sup>11,22–26</sup> EPR imaging is based on encoding spatial information in the EPR spectra via magnetic field gradients and provides information on the spatial properties of paramagnetic species in a nondestructive way. The combination of spectral information and spatial distribution of nitroxide spin probes in EPR imaging allows the detection of property changes in different parts of the examined system.<sup>27–29</sup> The development of low-frequency EPR spectrometers (1.1 GHz) now permits the noninvasive characterization of biodegradable DDS, such as PLGA and polyanhydride implants, *in vivo*.<sup>11,30–34</sup>

Poly(ortho esters) (POE) are a versatile family of biodegradable polymers that exhibit common characteristics such as hydrophobicity and acid-sensitive ortho ester linkages.<sup>35</sup> The latest family of POE contains either glycolic or lactic acid units in the polymer backbone.<sup>36–39</sup> A mechanistic understanding of polymer degradation pathways is critical in the development of biodegradable polymers. Recently, the degradation mechanism of POE containing lactic acid units in the polymer backbone was elucidated.<sup>40</sup> The concomitant linear weight loss and release of the degradation products lactic and propionic acids argues convincingly for a process confined predominantly to the surface layers of the polymer matrix. However, the process is not a pure surface erosion because a drop in molecular weight of the uneroded polymer is observed, indicating that some hydrolysis is taking place in the bulk material.

The objective of this study was to investigate further the *in vitro* degradation process by the direct and continuous determination of pH values inside the eroding POE by EPR imaging. Low molecular weight POE containing 30 mol % lactic acid units in the polymer backbone (POE<sub>70</sub>LA<sub>30</sub>) were selected for this study since they are currently investigated in ophthalmology, dentistry, and veterinary medicine.<sup>41</sup>

## Experimental Section

**Materials.** 1,10-Decanediol was purchased from Aldrich Chemie (Steinheim, Germany). D,L-Lactide was supplied by PURAC biochem (Gorinchem, The Netherlands). Triethylamine (TEA), 1-decanol, and *p*-toluenesulfonic acid (*p*-TSA) were purchased from Fluka Chemie AG (Buchs, Switzerland). 3,9-Diethylidene-2,4,8,10-tetraoxaspiro[5.5]undecane (DETOSU) was supplied by A.P. Pharma (Redwood City, CA). Nitroxide spin probes 4-amino-2,2,5,5-tetramethyl-3-imidazoline-1-yloxy (AT), 2,2,3,4,4,5,5-hexamethylimidazolidine-1-yloxy

(HM), and 2,2,4,5,5-pentamethyl-3-imidazoline-1-yloxy (PI) were purchased from Magnettech (Berlin, Germany). All solvents used were of analytical grade and purchased from SDS (Peypin, France).

### Synthesis and Characterization of Poly(ortho esters).

Low molecular weight POE<sub>70</sub>LA<sub>30</sub> were prepared by the acid-catalyzed condensation of DETOSU with 1,10-decanediol, 1,10-decanediol lactate, and 1-decanol as previously described by Schwach-Abdellaoui et al.<sup>39</sup> Average molecular weights were determined by size exclusion chromatography (SEC) using a Waters 515 HPLC pump E (Ruppertswil, Switzerland) with four Waters-Styragel HR 1-4 columns as stationary phase, a Waters 717 plus Auto-sampler, and a Waters 410 differential refractometer. The mobile phase was THF circulating at 1 mL/min. Samples were prepared by dissolution of the polymer in THF (5 mg/mL) and filtration through a 0.45  $\mu$ m Millipore filter (Milford, MA). A calibration curve was constructed using TSK polystyrene standards (Tosoh Corp., Tokyo, Japan) having molecular weights between 500 and 37 900 Da.

**pH Calibration Measurements.** Nitroxide spin probes (AT, HM, PI) were calibrated in citrate and phosphate buffer solutions in order to cover a pH range between 1.0 and 8.0. Nitroxide spin probes were dissolved in buffer solutions (100 mL), giving a final concentration of 5 mM. The pH value was adjusted by addition of either 0.1 M HCl or 0.1 M NaOH. For solutions with pH < 2, concentrated HCl was used. The pH was measured by means of a glass electrode (WTW pH 552, Weilheim, Germany). Aliquots of 1 mL were placed in thin-walled quartz tubes and inserted in the EPR cavity. EPR spectra were recorded as the first derivative of the absorption signal, and the hyperfine splitting  $a_N$  was measured as the distance between the low-field ( $m_I = +1$ ) and central ( $m_I = 0$ ) lines. Nitroxide spin probes were also calibrated in citrate and phosphate buffer solutions containing POE<sub>70</sub>LA<sub>30</sub> degradation products. This was achieved by placing 100 mg of POE<sub>70</sub>LA<sub>30</sub> in 100 mL of distilled water at 37 °C under agitation. After complete degradation of the polymer, 5 mL of the aqueous solution containing the degradation products were mixed with 5 mL of citrate and phosphate buffers. Nitroxide spin probes were dissolved in the solutions, giving a final concentration of 5 mM, and EPR spectra were recorded as described above.

**Experimental Settings for EPR.** EPR spectra were recorded at 25 °C at a frequency of 9.4 GHz using an X-band ERS 220 spectrometer (ZWG, Berlin, Germany) with a custom-made tomography extension, equipped with a rectangular resonator. The EPR parameters used were as follows: microwave power, 2 mW; modulation amplitude, 0.1 mT; scan width, 10 mT; maximum gradient, 4.27 T/m; scan time per projection, 10 s; 95 projections with 512 points per projection; image matrix, 256  $\times$  256 points. Images were calculated from the recorded set of EPR spectra by means of deconvolution and image reconstruction.

**Sample Preparation.** Nitroxide spin probes were incorporated separately in POE<sub>70</sub>LA<sub>30</sub> using the solvent evaporation technique according to Mäder et al.<sup>33</sup> Briefly, an ethanolic solution of each spin probe was prepared at a concentration of 1% (w/v). Then, defined volumes of spin probes in ethanolic solution were separately incorporated into POE<sub>70</sub>LA<sub>30</sub> to achieve a final nitroxide concentration of 5 mmol/kg. After incorporation of the spin probe solutions and homogenization, solvent was eliminated at 40 °C under vacuum for 4 h. Average polymer molecular weights were determined by SEC, as previously described, immediately after the incorporation of the spin probes and after 30 days of storage at 4 °C to check the stability of the polymer in the presence of the spin probes.

**Sample Incubation.** After the incorporation of spin probes in POE<sub>70</sub>LA<sub>30</sub>, samples (40 mg) were placed in EPR sample holders made of poly(ether ether ketone) (PEEK) (diameter 4 mm; depth 4 mm) and closed with a poly(ether sulfone) membrane with a pore size of 220 nm. The sample holders were placed in 0.1 M phosphate buffer (pH 7.4) at 37 °C under agitation, and the buffer was changed daily. At regular time intervals, samples were removed, and the water film at the surface was removed by blotting carefully with an absorbent paper before placing them in the resonator for EPR measure-

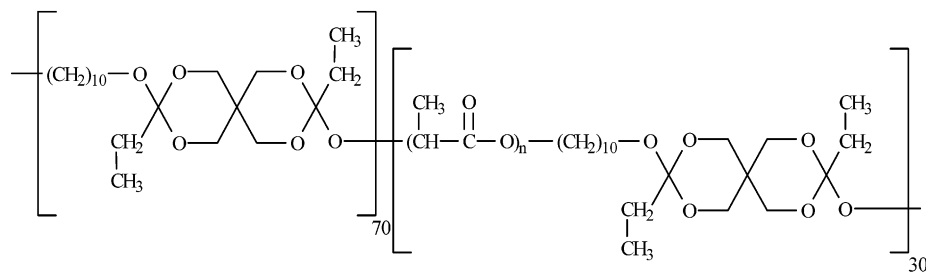


**Figure 1.** Structure of low molecular weight autocatalyzed POE<sub>70</sub>LA<sub>30</sub>.

ments. The pH values inside the eroding polymer samples were obtained from the calibration curves.

## Results and Discussion

**Synthesis and Characterization of Poly(ortho esters).** The structure of autocatalyzed POE<sub>70</sub>LA<sub>30</sub> is shown in Figure 1. The synthesis and characterization of POE<sub>70</sub>LA<sub>30</sub> by <sup>1</sup>H NMR, <sup>13</sup>C NMR, and FT-IR have been reported earlier.<sup>38,39</sup> Since degradation of bioerodible polymers depends mainly on composition, molecular weight, and molecular weight distribution, it is important to control the polycondensation reaction in order to synthesize low molecular weight POE<sub>70</sub>LA<sub>30</sub> in a reproducible manner. This can be achieved by the use of 1-decanol (15 mol %) during the polymerization reaction acting as a chain stopper.<sup>39</sup> Average molecular weights were determined by SEC, and results showed that the average molecular weight (*M<sub>w</sub>*) and polydispersity index (*M<sub>w</sub>*/*M<sub>n</sub>*) of POE<sub>70</sub>LA<sub>30</sub> were 6000 Da and 1.6, respectively.

**pH Calibration Measurements.** The calibration experiments demonstrated the expected pH sensitivity of the hyperfine splitting *a<sub>N</sub>*, as shown in Figure 2. All spectra consisted of the typical three-line pattern related to the hyperfine splitting *a<sub>N</sub>* of the <sup>14</sup>N atom in the spin probe. All three lines were almost equal in height and symmetry since there are no limitations for the mobility of the nitroxide spin probes in aqueous solutions. The pH sensitivity of nitroxide spin probes is based on pH-induced changes in the spin density of the nitroxide group: protonation of the nitrogen atom at position 3, shown in Figure 3, leads to a decrease in the spin density on the nitrogen atom in position 1, which results in a decreased hyperfine splitting *a<sub>N</sub>* and an increased *g*-factor.<sup>18</sup> The calibration curves were established by a sigmoidal Boltzmann fit to the values of the hyperfine splitting. The *pK<sub>a</sub>* values obtained from the calibration curves for AT, HM, and PI were 6.1, 4.7, and 1.8, respectively (*r*<sup>2</sup> > 0.993). The *pK<sub>a</sub>* values of these radicals largely depend on the type of substituent in position 4, and the results are in good agreement with previously published results.<sup>24,28,29</sup> The calibration experiments performed in the presence of polymer degradation products did not show significant shifts in *pK<sub>a</sub>* values. The hyperfine splitting *a<sub>N</sub>* of AT, HM, and PI measured inside the eroding POE<sub>70</sub>LA<sub>30</sub> samples by EPR were used for the determination of pH values, with an accuracy of ±0.05 pH units. Only pH values measured in the range of *pK<sub>a</sub>* ± 1 pH unit of the nitroxide spin probes were taken into consideration in the erosion experiments.

**Erosion Experiments.** The application of EPR to study the degradation process of polymeric biomaterials composed of diamagnetic species is only possible after the incorporation of paramagnetic compounds, i.e., spin probes. The incorporation procedure of nitroxide spin

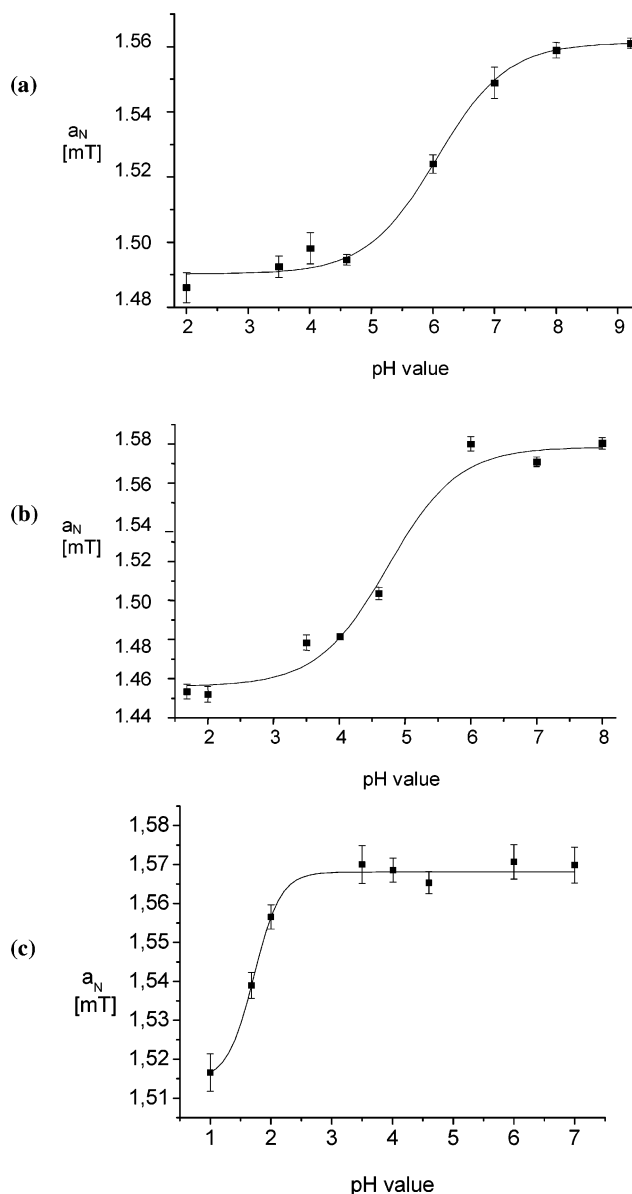


**Figure 2.** pH sensitivity of the hyperfine splitting *a<sub>N</sub>* of AT (a), HM (b), and PI (c) nitroxide spin probes measured by EPR spectroscopy (9.4 GHz).

probes AT, HM, and PI in the polymer samples did not induce degradation. The average molecular weight remained constant during 30 days of storage at 4 °C, as determined by SEC measurements.

Since low molecular weight autocatalyzed POE<sub>70</sub>LA<sub>30</sub> have a viscous consistency at ambient temperature, it was difficult to fill the standard quartz tubes used in the calibration experiments. Therefore, we designed new poly(ether ether ketone) (PEEK) sample holders. PEEK



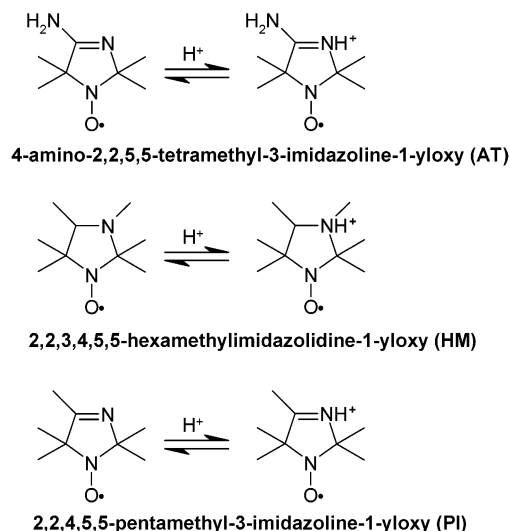


**Figure 3.** Structures and pH sensitivity of selected nitroxide spin probes.

is a semicrystalline polymer exhibiting exceptional properties including excellent mechanical properties, good chemical and fatigue resistance, and high temperature durability. In addition, PEEK can be easily processed using conventional plastic processing equipment. The PEEK sample holders (diameter 4 mm; depth: 4 mm) were developed in order to perform the incubation experiments in 0.1 M phosphate buffer (pH 7.4) at 37 °C under agitation and to record EPR spectra at selected time intervals in the same sample holder without sample handling. Polymer samples (40 mg) were placed in the specially designed EPR sample holders and closed with a poly(ether sulfone) membrane with a pore size of 220 nm.

Before incubation in phosphate buffer, EPR spectra were recorded at 25 °C to evaluate the distribution of nitroxide spin probes in the POE<sub>70</sub>LA<sub>30</sub> samples. All spectra recorded before incubation showed homogeneous distributions of the spin probes in the amorphous POE<sub>70</sub>LA<sub>30</sub>. A representative EPR image obtained after the incorporation of PI nitroxide spin probe is shown in Figure 4. As illustrated, images displaying spectral properties as a function of their distribution along one spatial axis are achieved. The image corresponds to a model object, the coordinates of which are length, field, and signal amplitude. Nitroxide spin probes tumble in aqueous solutions or other nonviscous solvents giving highly symmetric spectra, as observed in the calibration experiments. Higher viscosity results in less averaging of the anisotropy, increased line widths, and decreased signal amplitude, particularly of the first and third lines. All spectra recorded before incubation confirmed the reduced mobility of the nitroxide spin probes when incorporated in the viscous POE<sub>70</sub>LA<sub>30</sub>, as observed in Figure 4.

Polymer samples were incubated in 0.1 M phosphate buffer (pH 7.4) at 37 °C under agitation and were removed for EPR measurements at selected time intervals. After 15 h of incubation, differences in the spectral shape between the outer layers and the core of the sample started to develop, as illustrated in Figure 5 (upper row). The surface of the polymer sample that was in contact with buffer (i.e., area close to the membrane at 3.8 mm) showed a significantly higher signal amplitude, due to enhanced mobility and line narrowing resulting from water diffusion, when compared to the core of the sample. During the first 7 days of incubation, only small changes in signal amplitudes in the surface layer of the polymer samples occurred (Figure 5, middle row). The lack of any changes in the core of the sample

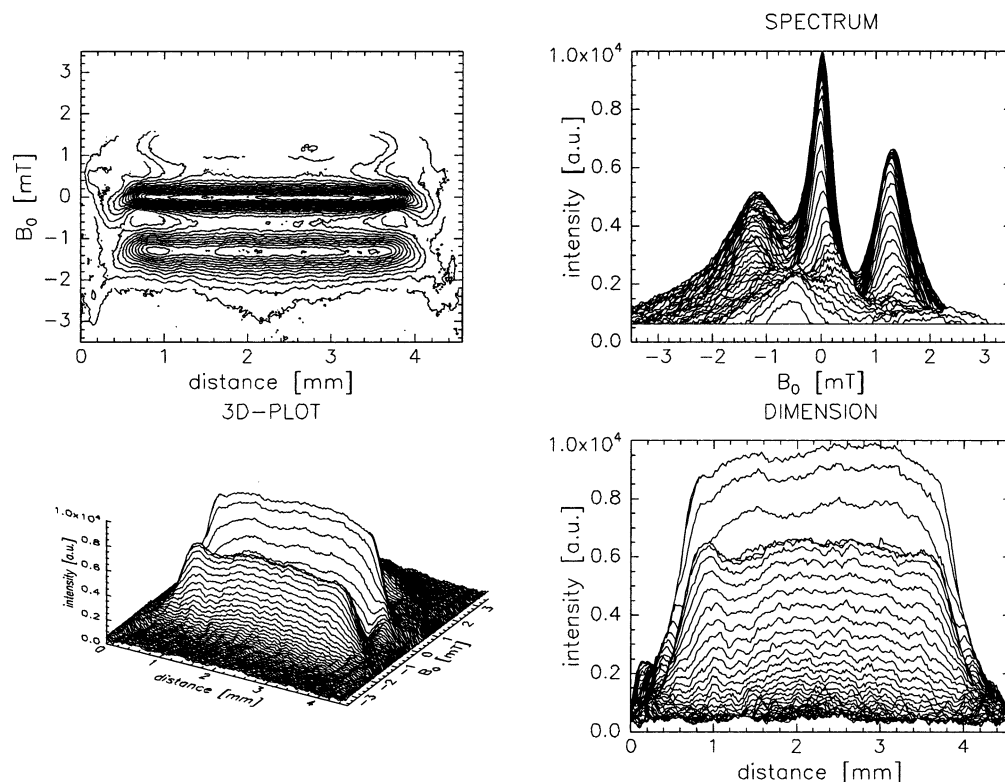


**Figure 4.** Representative EPR images obtained after the incorporation of nitroxide spin probe PI in the viscous POE<sub>70</sub>LA<sub>30</sub>. From left to right: top view; spectral view (from the bottom of the PEEK sample holder to the membrane); 3D plot; dimensional view (0 mm: bottom of the PEEK sample holder; 4 mm: membrane).

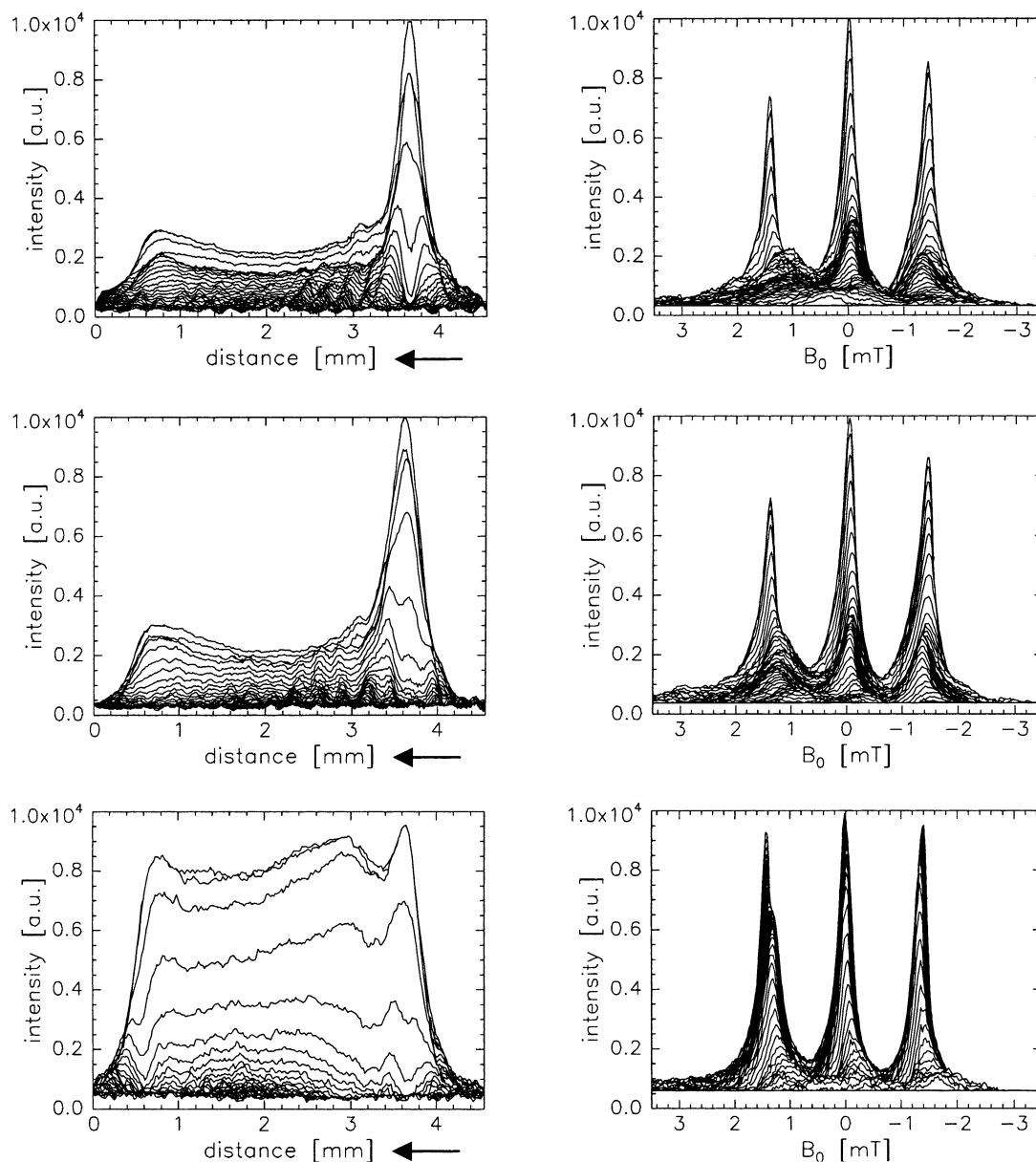


**Figure 5.** EPR images of PI nitroxide spin probe in POE<sub>70</sub>LA<sub>30</sub> obtained after 15 h (upper row), 168.5 h (middle row), and 195 h (bottom row) of incubation in 0.1 M phosphate buffer (pH 7.4) at 37 °C. From left to right: dimensional view (0 mm: bottom of the PEEK sample holder; 4 mm: membrane; the arrow indicates the direction of the diffusion front); spectral view (from the bottom of the PEEK sample holder to the membrane).

during the first week of incubation was due to either the absence of water penetration during this time or any penetrating water becoming tightly bound. In consequence, during the first phase of degradation the measurement of pH values was only possible in the surface layer of the polymer samples, where sufficient water could penetrate to hydrolyze the ester bonds generating carboxylic end groups; pH values between 6.0 and 7.4 were recorded in the surface layer of POE<sub>70</sub>LA<sub>30</sub>. With time, diffusion of water into the core of the sample increased, and the spectral contribution of rapidly tumbling nitroxide spin probes, characterized by a spectrum of three narrow lines, became predominant as illustrated in Figure 5 (bottom row). The EPR image clearly showed enhanced signal amplitudes throughout the sample due to enhanced mobility of the spin probes, allowing the determination of pH values inside the eroding POE<sub>70</sub>LA<sub>30</sub> from day 7 until complete erosion. After 195 h of incubation in 0.1 M phosphate buffer (pH 7.4) at 37 °C (Figure 5, bottom row), the

spectral contribution of rapidly tumbling PI spin probe became predominant. The time needed for the predominance of rapidly tumbling spin probes was spin probe dependent since nitroxides spin probes have different characteristics (molecular weight,  $pK_a$ ,  $\log P$ ). The rapid change in EPR spectra occurring between 168.5 and 195 h was surprising, and the reason for this rapid change is yet unknown. The incorporation of different spin probes, such as 3-carbamoyl-2,2,5,5-tetramethylpyrrolidine-1-yloxy (PCM), into POE<sub>70</sub>LA<sub>30</sub> might elucidate this phenomenon. Indeed, PCM has been incorporated into biodegradable polymers to quantify the changes in viscosity, resulting from water diffusion.<sup>34</sup> Magnetic resonance imaging can also be applied to monitor and quantify the hydration process and to characterize the state of water in terms of proton relaxation times or self-diffusion coefficients.<sup>11</sup> The use of both noninvasive imaging techniques can give complementary information to understand and quantify the mechanisms of poly(ortho ester) degradation.

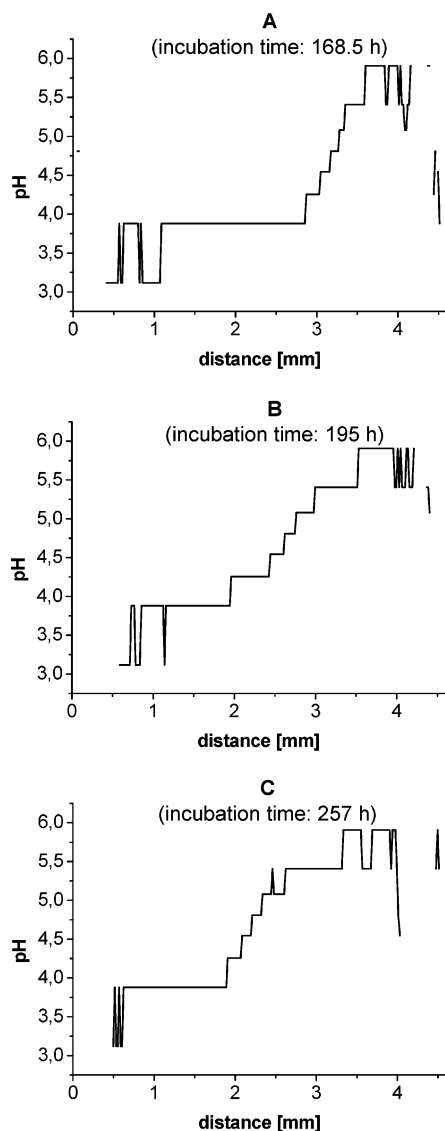


**Figure 6.** Experimental pH values measured inside the eroding POE<sub>70</sub>LA<sub>30</sub> after (A) 168.5, (B) 195, and (C) 257 h of incubation in 0.1 M phosphate buffer (pH 7.4) at 37 °C.

As can be seen in Figure 6, the first measurement of pH inside the eroding POE<sub>70</sub>LA<sub>30</sub> indicated a value of 3.8 in the core of the sample and a higher pH in the surface layers (Figure 6A). The accumulation of acidic degradation products, which cannot freely diffuse out of the sample, was responsible for the observed pH drop inside eroding POE<sub>70</sub>LA<sub>30</sub>, even when 0.1 M phosphate buffer (pH 7.4) was used. It was also possible to observe a polymer erosion front moving down within the polymer matrix in the course of time, as shown in Figure 6B,C. The pH value of 3.8 measured inside the eroding POE<sub>70</sub>LA<sub>30</sub> did not change until polymer samples disintegrated at day 23. These results demonstrate the importance of solubility of the degradation products in the degradation process. After 23 days of incubation in 0.1 M phosphate buffer (pH 7.4) at 37 °C, no EPR signal was detectable.

Consequently, our results suggest that the *in vitro* degradation of low molecular weight POE<sub>70</sub>LA<sub>30</sub> followed a two-phase process: in the first week of incubation, diffusion of water was limited to the surface layer of the sample (i.e., less than 1 mm), which confirmed that POE<sub>70</sub>LA<sub>30</sub> are hydrophobic biomaterials. The

water molecules in the surface layer of the polymer started to hydrolyze the ester bonds, generating polymer fragments containing carboxylic acid end groups, which further catalyze the cleavage of ester and ortho ester bonds. The lowest pH value measured in the surface layer was 6.0, since acidic degradation products were able to leach out of the sample holder. After 1 week of incubation in 0.1 M phosphate buffer (pH 7.4) at 37 °C, water diffused into the polymer bulk and started the cleavage of ester bonds in the bulk material, as described above. The observed pH drop to values as low as 3.8 after 1 week of incubation in 0.1 M phosphate buffer (pH 7.4) confirmed the autocatalytic degradation process of POE<sub>70</sub>LA<sub>30</sub> described by Schwach-Abdellaoui et al.<sup>40</sup> Indeed, it has been shown that the *in vitro* hydrolysis proceeds in several steps; in the first step, the lactic acid units in the polymer backbone hydrolyze to generate polymer fragments containing carboxylic acid end groups, which will catalyze the hydrolysis of ester and ortho ester bonds. A second cleavage produces lactic acid, which also catalyzes hydrolysis of the ortho ester bonds. Further hydrolysis of ortho ester bonds then proceeds in two steps to generate first 1,10-decanediol, 1-decanol, and pentaerythritol dipropionate, followed by ester hydrolysis to produce pentaerythritol and propionic acid. The data obtained from the changes in molecular weight, kinetics of weight loss, and release of lactic acid and propionic acid show that the erosion process of autocatalyzed POE is not a pure surface erosion because there is a significant drop in molecular weight of the uneroded polymer, indicating that hydrolysis is also taking place in the bulk material.<sup>40</sup>

It is important to keep in mind that the changes in pH values observed inside eroding DDS by EPR imaging are also dependent on the size of the DDS because clearance of acidic degradation end products is faster in smaller DDS due to shorter diffusion distances. In larger DDS, the diffusion distance is long enough to prevent the buffer from neutralizing the pH.<sup>10</sup> The appearance of a pH gradient, with lowest pH values at the center of the matrix and higher pH values near the surface, are consistent with a diffusion-controlled mechanism in which acidic degradation products initially diffuse out of the matrix very slowly.<sup>10,42</sup> Therefore, the degradation of the polymer matrix surface will be slower compared to the center. In summary, EPR imaging showed that the *in vitro* erosion mechanism of POE<sub>70</sub>LA<sub>30</sub> was neither bulk erosion nor pure surface erosion.<sup>43</sup>

Similar results were obtained by Mäder et al., who applied EPR imaging to characterize the *in vitro* degradation of polyanhydride disks in 0.1 M phosphate buffer (pH 7.4) at 37 °C.<sup>28</sup> Results also showed the formation of a front of degraded polymer in the disk from outside to inside. A pH gradient was found between the degrading polymer and the buffer, with the minimum pH as low as 4.0. However, lower pH values could not be observed inside the eroding DDS, since only the AT nitroxide spin probe was used in their study. In another study, implants of poly(DL-lactide-co-glycolide) (PLGA 50:50) were placed in living mice, and results showed that during the first days after implantation the mobility of the nitroxide spin probes was too limited to determine pH values. After a lag time of about 1 week, the recorded EPR spectra gave direct evidence for the formation of an acidic compartment within eroding implants with the minimum pH as low as 2.0.<sup>33</sup> The

formation of an acidic environment within eroding DDS may have significant effects on drug stability, bioavailability, pharmacokinetics, and therapeutic efficiency.

## Conclusions

Quantifying the pH environment inside eroding polymeric DDS is critical for furthering the understanding of polymer degradation and release kinetics and for optimizing the stability of the incorporated active compounds. EPR imaging allowed a noninvasive spatially resolved observation of pH changes within POE<sub>70</sub>LA<sub>30</sub>. Results showed that the in vitro degradation of POE<sub>70</sub>LA<sub>30</sub> is not a pure surface erosion process due to the introduction of lactic acid units in the polymer backbone. The pH changes observed during the in vitro autocatalytic degradation of POE<sub>70</sub>LA<sub>30</sub> suggest that autocatalyzed poly(ortho esters) are promising polymers for the controlled release of pH-sensitive compounds.

## References and Notes

- (1) Park, T. G.; Lu, W.; Crotts, G. *J. Controlled Release* **1995**, *33*, 211.
- (2) Tobio, M.; Alonso, M. J. *S.T.P. Pharma Sci.* **1998**, *8*, 303.
- (3) Anderson, J. M.; Langone, J. J. *J. Controlled Release* **1999**, *57*, 107.
- (4) Domb, A.; Turovsky, L.; Nudelman, R. *Pharm. Res.* **1994**, *11*, 865.
- (5) Cleland, J.; Powell, M.; Shire, S. *Crit. Rev. Ther. Drug Carrier Syst.* **1993**, *10*, 307.
- (6) Middaugh, C.; Evans, R.; Montgomery, D.; Casimiro, D. *J. Pharm. Sci.* **1998**, *87*, 130.
- (7) Tamada, J. A.; Langer, R. *Proc. Natl. Acad. Sci. U.S.A.* **1993**, *90*, 552.
- (8) Therin, M.; Christel, P.; Li, S.; Garreau, H.; Vert, M. *Biomaterials* **1992**, *13*, 594.
- (9) Shenderova, A.; Burke, T. G.; Schwendeman, S. P. *Pharm. Res.* **1999**, *16*, 241.
- (10) Fu, K.; Pack, D. W.; Klibanov, A. M.; Langer, R. *Pharm. Res.* **2000**, *17*, 100.
- (11) Mäder, K.; Crémilleux, Y.; Domb, A. J.; Dunn, J. F.; Swartz, H. M. *Pharm. Res.* **1997**, *14*, 820.
- (12) Burke, P. A. *Int. Symp. Controlled Release Bioact. Mater.* **1996**, *23*, 133.
- (13) Deutsch, C. J.; Taylor, J. S. *Ann. N.Y. Acad. Sci.* **1987**, *508*, 33.
- (14) Mäder, K.; Swartz, H. M.; Stösser, R.; Borchert, H. H. *Pharmazie* **1994**, *49*, 97.
- (15) Sintzel, M. B.; Schwach-Abdellaoui, K.; Mäder, K.; Stösser, R.; Heller, J.; Tabatabay, C.; Gurny, R. *Int. J. Pharm.* **1998**, *175*, 165.
- (16) Mäder, K.; Stösser, R.; Borchert, H. H.; Mank, R.; Nerlich, B. *Pharmazie* **1991**, *46*, 342.
- (17) Mäder, K.; Borchert, H. H.; Stösser, R.; Groth, N.; Herrling, T. *Pharmazie* **1991**, *46*, 439.

- (18) Khramtsov, V. V.; Weiner, L. M.; Grigoriev, I. A.; Volodarsky, L. B. *Chem. Phys. Lett.* **1982**, *91*, 69.
- (19) Khramtsov, V. V.; Panteleev, M. V.; Weiner, L. M. *J. Biochem. Biophys. Methods* **1989**, *18*, 237.
- (20) Khramtsov, V. V.; Marsh, D.; Weiner, L. M.; Reznikov, V. A. *Biochim. Biophys. Acta* **1992**, *1104*, 317.
- (21) Paschenko, S. V.; Dzuba, S. A.; Khramtsov, V. V.; Tsvetkov, Y. D. *Ber. Bunsen-Ges. Phys. Chem.* **1998**, *102*, 224.
- (22) Kroll, C.; Mäder, K.; Stösser, R.; Borchert, H. H. *Eur. J. Pharmacol. Sci.* **1995**, *3*, 21.
- (23) Mäder, K.; Bittner, B.; Li, Y.; Wohlauf, W.; Kissel, T. *Pharm. Res.* **1998**, *15*, 787.
- (24) Brunner, A.; Mäder, K.; Göpferich, A. *Pharm. Res.* **1999**, *16*, 847.
- (25) Witt, C.; Mäder, K.; Kissel, T. *Biomaterials* **2000**, *21*, 931.
- (26) Katzhendler, I.; Mäder, K.; Friedman, M. *Int. J. Pharm.* **2000**, *200*, 161.
- (27) Maltempo, M. M.; Eaton, S. S.; Eaton, G. R. In *EPR Imaging and In Vivo EPR*; Eaton, G. R., Eaton, S. S., Ohno, K., Eds.; CRC Press: Boca Raton, FL, 1991; p 135.
- (28) Mäder, K.; Nitschke, S.; Stösser, R.; Borchert, H. H.; Domb, A. *Polymer* **1997**, *38*, 4785.
- (29) Kroll, C.; Herrmann, W.; Stösser, R.; Borchert, H. H.; Mäder, K. *Pharm. Res.* **2001**, *18*, 525.
- (30) Swartz, H. M.; Bacic, G.; Gallez, B.; Goda, F.; James, P.; Jiang, J.; Liu, K. J.; Mäder, K.; Nakashima, T.; O'Hara, J.; Shima, T.; Walczak, T. In *Bioradicals Detected by EPR Spectroscopy*; Ohya-Nishiguchi, H., Packer, L., Eds.; Birkhäuser Verlag: Basel, 1995; p 285.
- (31) Stösser, R.; Mäder, K.; Borchert, H. H.; Herrmann, W.; Schneider, G.; Liero, A. In *Bioradicals Detected by ESR Spectroscopy*; Ohya-Nishiguchi, H., Packer, L., Eds.; Birkhäuser Verlag: Basel, 1995; p 301.
- (32) Gallez, B.; Mäder, K.; Swartz, H. M. *Magn. Reson. Med.* **1996**, *36*, 694.
- (33) Mäder, K.; Gallez, B.; Liu, K. J.; Swartz, H. M. *Biomaterials* **1996**, *17*, 457.
- (34) Mäder, K.; Bacic, G.; Domb, A.; Elmalak, O.; Langer, R.; Swartz, H. M. *J. Pharm. Sci.* **1997**, *86*, 126.
- (35) Heller, J.; Barr, J.; Ng, S. Y.; Schwach-Abdellaoui, K.; Gurny, R. *Adv. Drug Deliv. Rev.* **2002**, *54*, 1015.
- (36) Ng, S. Y.; Vandamme, T.; Taylor, M. S.; Heller, J. *Macromolecules* **1997**, *30*, 770.
- (37) Sintzel, M. B.; Heller, J.; Ng, S. Y.; Taylor, M. S.; Tabatabay, C.; Gurny, R. *Biomaterials* **1998**, *19*, 791.
- (38) Schwach-Abdellaoui, K.; Heller, J.; Gurny, R. *J. Biomater. Sci., Polym. Ed.* **1999**, *10*, 375.
- (39) Schwach-Abdellaoui, K.; Heller, J.; Barr, J.; Gurny, R. *Int. J. Polym. Anal. Charact.* **2002**, *7*, 145.
- (40) Schwach-Abdellaoui, K.; Heller, J.; Gurny, R. *Macromolecules* **1999**, *32*, 301.
- (41) Einmahl, S.; Capancioni, S.; Schwach-Abdellaoui, K.; Moeller, M.; Behar-Cohen, F.; Gurny, R. *Adv. Drug Deliv. Rev.* **2001**, *53*, 45.
- (42) Siepmann, J.; Göpferich, A. *Adv. Drug Deliv. Rev.* **2001**, *48*, 229.
- (43) Von Burkersroda, F.; Schedl, L.; Göpferich, A. *Biomaterials* **2002**, *23*, 4221.

MA034365Q